Photoredox Properties of Homoleptic d^6 Metal Complexes with the Electron-Rich 4,4‘,5,5‘-Tetramethoxy-2,2‘-Bipyridine Ligand

Laura A. Büldt,[a] Alessandro Prescimone,[a] Markus Neuburger,[a] and Oliver S. Wenger*[a]

Abstract: A synthetic procedure leading to 4,4',5,5'-tetramethoxy-2,2'-bipyridine ((MeO)$_4$bpy) was developed, and the first three metal complexes with this ligand were synthesized. A few ligand precursor compounds, the final ligand, and its homoleptic iron(II) complex were characterized structurally by X-ray diffraction. The combination of cyclic voltammetry, optical absorption, luminescence, and transient absorption spectroscopy provided detailed insight into the electronic structure of the entire series of homoleptic Fe(II), Ru(II), and Os(II) complexes. The ruthenium(II) complex is a more potent photoreductant than the [Ru(2,2'-bipyridine)$_3$]$^{2+}$ parent compound by approximately 0.4 V as confirmed by ^{3}MLCT excited-state quenching experiments with a relatively mild oxidant, 1-chloro-4-nitrobenzene. In presence of methanesulfonic acid in CH_3CN, the photoexcited [Ru((MeO)$_4$bpy)$_3$]$^{2+}$ complex is able to undergo proton-coupled electron transfer (PCET) with acetophenone to yield a ketyl radical. Chemically robust and potent photoreductants are of interest for phototriggering of electron transfer reactions, for example in photoredox catalysis, in dye-sensitized solar cells, in fundamental studies of (proton-coupled) electron transfer, or for the generation of solvated electrons.

Introduction

Complexes of d^6 metals with α-diimine ligands are a very well investigated class of materials.[1] From a photophysical and photochemical perspective, ruthenium(II) and osmium(II) α-diimines are attractive due to their relatively long-lived and emissive ^{3}MLCT excited states in which the redox properties are drastically altered when compared to the electronic ground state.[2] Cyclometalated iridium(III) complexes and rhenium(I) tricarbonyl diimines exhibit similarly favorable electronic structures in many cases.[3] Consequently, such d^6 metal complexes have found use in various applications, ranging for example from luminescent materials to sensors,[4] dyes for solar cells,[5] DNA intercalators,[6] and photosensitizers for electron or energy transfer processes.[7] Recently, these types of complexes have received significant attention in the context of photoredox catalysis and small molecule activation.[8] Furthermore, electron-rich Ru(α-diimine)$_3^{2+}$ complexes have become of interest for the photogeneration of solvated electrons.[9]

[a] L. A. Büldt, Dr. A. Prescimone, Dr. M. Neuburger, Prof. Dr. O. S. Wenger
Department of Chemistry
University of Basel
St. Johanns-Ring 19, CH-4056 Basel, Switzerland
E-mail: oliver.wenger@unibas.ch

Supporting information for this article is given via a link at the end of the document.

As part of our research program on long-range electron tunneling and proton-coupled electron transfer (PCET) we were interested in robust d^6 metal diimine complexes which are potent electron donors in their long-lived ^{3}MLCT excited states.[10] The electrochemical potentials and MLCT energies of such complexes are commonly tuned by ligand variation. A very simple strategy is to introduce electron-donating or electron-withdrawing substituents,[1] and there has been much fundamental work on how such ligand modifications alter the electrochemical and photophysical properties.[11] The largest and most important ligand family in this context is based on the 2,2'-bipyridine (bpy) parent ligand. Numerous variants of bpy are known, and most of them are symmetrical 4,4'-, 5,5'-, or 6,6'-di-substituted ligands while tetra-substituted versions are less common.[1] To our knowledge, the 4,4',5,5'-tetramethoxy-2,2'-bipyridine ((MeO)$_4$bpy) molecule, although reported in 1995 as part of a synthetic effort on pyridines,[12] had never been used as a ligand to any metal until now. Given the electron-donating nature of methoxy-substituents and their high chemical robustness (for example when compared to dimethylamino-groups),[13] we anticipated d^6 metal complexes with comparatively low oxidation potentials which might be particularly potent reductants in their long-lived ^{3}MLCT excited states.

We report here an efficient new procedure for the synthesis of (MeO)$_4$bpy and present the first complexes made with this ligand. Specifically, we focused on the homoleptic complexes of iron(II), ruthenium(II), and osmium(II). Crystal structures of the free ligand, the [Fe((MeO)$_4$bpy)$_3$]$^{2+}$ complex, and some ligand precursor molecules have been obtained. The electrochemical and photophysical properties of the complexes were explored in detail, and we find that [Ru((MeO)$_4$bpy)$_3$]$^{2+}$ is indeed a very potent excited-state electron donor. The redox and photophysical properties of the new complexes are rationalized by comparison with existing data of related bpy-based complexes.

Results and Discussion

Synthesis. Commercial 2-chloro-5-aminopyridine (**1**) was reacted with $NaNO_2$ in diluted sulfuric acid, and after neutralization with aqueous Na_2CO_3 2-chloro-5-hydroxypyridine (**2**) was isolated (Scheme 1).[14] The latter was converted to 2-chloro-5-methoxypyridine (**3**) with iodomethane in presence of K_2CO_3. Using urea·H_2O_2 adduct and trifluoroacetic anhydride, conversion to 2-chloro-5-methoxypyridine-*N*-oxide (**4**) occurred.[15] Subsequent reaction in nitrating acid gave 2-chloro-4-nitro-5-methoxypyridine (**5**), i. e., nitration and loss of the *N*-oxide occurred in the same reaction step. Treatment of molecule **5** with tetrabutylammonium methanolate in THF afforded 2-

chloro-4,5-dimethoxypyridine (**6**).[16] A homocoupling reaction catalyzed by $Ni(PPh_3)_2Cl_2$ in the presence of Zn powder and tetrabutylammonium iodide gave the final 4,4',5,5'-tetramethoxy-2,2'-bipyridine ligand (**7**, $(MeO)_4bpy$).[17] The overall yield for the 6 reaction steps from molecule **1** to ligand **7** was 6 %. This newly developed procedure is significantly different from the only previously published protocol for the synthesis of 4,4',5,5'-tetramethoxy-2,2'-bipyridine and in our hands proved to be more effective.[12]

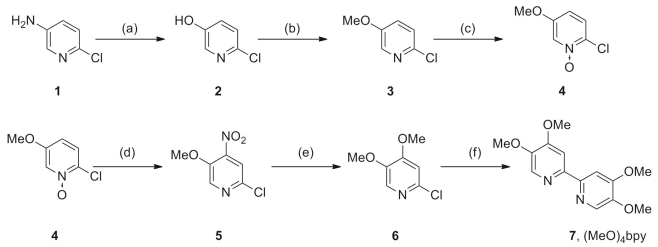

Scheme 1. Synthetic steps leading to the 4,4',5,5'-tetramethoxy-2,2'-bipyridine ligand (**7**, $(MeO)_4bpy$). (a) $NaNO_2$, dil. H_2SO_4, conc. AcOH, then aq. Na_2CO_3; (b) CH_3I, K_2CO_3, dry CH_3CN; (c) urea·H_2O_2, trifluoroacetic anhydride, CH_2Cl_2; (d) conc. H_2SO_4, conc. HNO_3; (e) $TBAOCH_3$, THF; (f) $Ni(PPh_3)_2Cl_2$, Zn, Et_4NI, THF.

The metal complexes were synthesized with standard methods, using $Fe(BF_4)_2·6H_2O$, $RuCl_3·0.5\ H_2O$, and $(NH_4)_2OsCl_6$ as metal sources. The final complexes as well as ligand **7** ($(MeO)_4bpy$) were fully characterized by ^1H and ^{13}C NMR, high-resolution mass spectrometry, and elemental analysis. Complete synthetic protocols and product characterization data are in the experimental section. ^1H NMR spectra of all compounds are in the supporting information (Figure S1-S9).

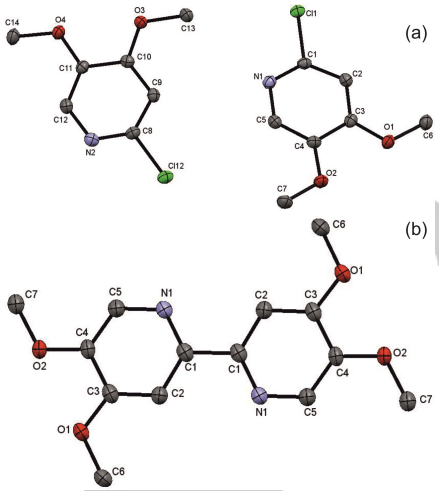

Figure 1. (a) Crystallographic structure of two 2-chloro-4,5-dimethoxypyridine (**6**) molecules forming the asymmetric unit. (b) Crystallographic structure of the 4,4',5,5'-tetramethoxy-2,2'-bipyridine ligand (**7**, $(MeO)_4bpy$). Anisotropic displacement parameters are drawn at the 50% probability level.

Crystallographic studies. In Figure 1a two molecules of 2-chloro-4,5-dimethoxypyridine (**6**) as found in the asymmetric unit of an X-ray crystal structure are shown. The crystallographic structure of 4,4',5,5'-tetramethoxy-2,2'-bipyridine (**7**, $(MeO)_4bpy$) is shown in Figure 1b. In both structures the methoxy-groups are nearly coplanar with the pyridine rings, and in $(MeO)_4bpy$ the two pyridine moieties are essentially coplanar with one another, but with N-atoms on opposite sides, as commonly observed for bpy ligands. An X-ray crystal structure of 2-chloro-4-nitro-5-methoxypyridine (**5**) is shown in the supporting information (Figure S10).

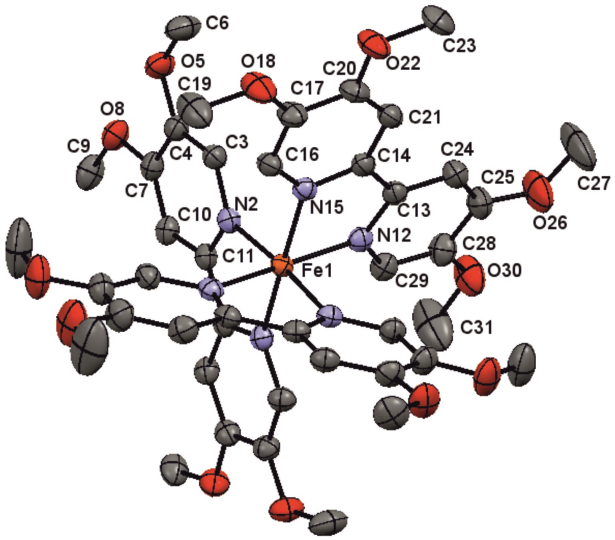

Figure 2. Crystallographic structure of the $[Fe((MeO)_4bpy)_3]^{2+}$ cation. Anisotropic displacement parameters are drawn at the 50% probability level.

The homoleptic d^6 metal complexes with $(MeO)_4bpy$ were more tricky to crystallize. With BF_4^- and PF_6^- anions the resulting crystals were not of sufficient quality for X-ray diffraction experiments, only with triflate we obtained a satisfactory result. The respective crystals were obtained by diffusion of diethyl ether vapor into acetonitrile solution. In Figure 2 the crystallographic structure of the $[Fe((MeO)_4bpy)_3]^{2+}$ cation is shown. The methoxy-substituents remain essentially coplanar with the pyridine rings to which they are attached. Complete crystallographic details are included in the experimental section and in the supporting information.

Electrochemistry. Cyclic voltammetry of the $[Fe((MeO)_4bpy)_3]^{2+}$, $[Ru((MeO)_4bpy)_3]^{2+}$, and $[Os((MeO)_4bpy)_3]^{2+}$ complexes was performed in dry CH_3CN with 0.1 M $TBAPF_6$. The results are shown in Figure 3 (solid lines). Voltammograms recorded for the $[Fe(bpy)_3]^{2+}$, $[Ru(bpy)_3]^{2+}$ and $[Os(bpy)_3]^{2+}$ reference complexes were measured under identical conditions and are included in Figure 3 (dashed traces). All redox potentials extracted from Figure 3 are summarized in Table 1 along with those of some related homoleptic Ru(II) complexes (values taken from the literature). For all three metals (M) considered here, the M^{3+}/M^{2+}

reduction potential is roughly 0.4 V lower for L = $(MeO)_4$bpy than for L = bpy (second column of Table 1). The $[Fe((MeO)_4bpy)_3]^{2+}$ complex becomes unstable upon reduction hence the observation of only one single irreversible reduction wave instead of three reversible waves, as is usually the case for homoleptic d^6 metal complexes with bpy ligands. For the Ru(II) and Os(II) complexes each of the three subsequent one-electron reductions of individual ligands occurs at potentials more negative by about 0.3 V in complexes with L = $(MeO)_4$bpy when compared to L = bpy.

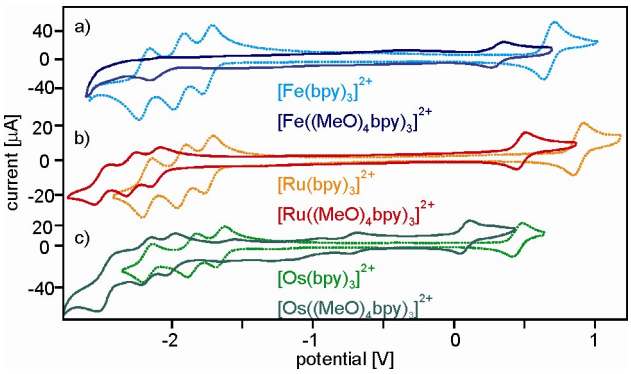

Figure 3. Cyclic voltammograms of the $[M((MeO)_4bpy)_3]^{2+}$ and $[M(bpy)_3]^{2+}$ complexes in CH_3CN with 0.1 M $TBAPF_6$. The scan rate was 0.2 V/s, the potential is reported versus the ferrocenium/ferrocene (Fc^+/Fc) couple.

Table 1. Reduction potentials (in Volts vs. Fc^+/Fc) for the various metal- and ligand-based electrochemical processes of the three key complexes and some relevant reference complexes.

complex	$E^0(M^{3+/2+})$	$E^0(L/L^-)$[b]	$E^0(L^-/L^{2-})$[c]	$E^0(L^{2-}/L^{3-})$
$[Fe(bpy)_3]^{2+}$	0.71[a]	-1.75[a]	-1.95[a]	-2.19[a]
$[Fe((MeO)_4bpy)_3]^{2+}$	0.31[a]			
$[Ru(bpy)_3]^{2+}$	0.89[a]	-1.72[a]	-1.91[a]	-2.15[a]
$[Ru(4,4'\text{-}Me_2bpy)_3]^{2+}$	0.75[b]	-1.75[b]	-1.92[b]	-2.18[b]
$[Ru(4,4'\text{-}{}^tBu_2bpy)_3]^{2+}$	0.73[c]	-1.82[c]		
$[Ru(4,4',5,5'\text{-}Me_4bpy)_3]^{2+}$	0.68[b]	-1.87[b]	-2.08[b]	-2.37[b]
$[Ru(4,4'\text{-}(MeO)_2bpy)_3]^{2+}$	0.56[d]	-1.87[d]	-2.04[d]	-2.24[d]
$[Ru((MeO)_4bpy)_3]^{2+}$	0.47[a]	-2.01[a]	-2.18[a]	-2.46[a]
$[Ru(4,4'\text{-}Me_2N)_2bpy)_3]^{2+}$	-0.05[e]			
$[Os(bpy)_3]^{2+}$	0.45[a]	-1.67[a]	-1.86[a]	-2.16[a]
$[Os((MeO)_4bpy)_3]^{2+}$	0.08[a]	-2.01[a]	-2.18[a]	-2.46[a]

[a] Measured in this work (Figure 3) in CH_3CN with 0.1 M $TBAPF_6$ using scan rates of 0.2 V/s. [b] From ref. [18]. [c] From ref. [19]. [d] From ref. [13a]. [e] From ref. [20]. Literature potentials reported against reference electrodes other than Fc^+/Fc were converted to Fc^+/Fc using the conversion constants reported earlier.[21]

Several Ru(II) complexes with 4,4'-disubstituted and 4,4',5,5'-tetrasubstituted bpy ligands have been previously characterized electrochemically, hence for this metal one can put the effect of the fourfold methoxyl-substitution into broader and more quantitative perspective (Table 1). Substitution at the 4- and 4'-positions with methyl- and *tert.*-butyl groups lowers the M^{3+}/M^{2+} reduction potential by roughly 0.15 V compared to ordinary bpy,[18-19] while the use of two methoxy-groups causes a lowering by 0.3 V.[13a] The effect of additional substitution at the 5- and 5'-positions in $(MeO)_4$bpy therefore is relatively small, only about 0.1 V, to cause a total shift of 0.4 V. This is not unexpected as substituents in *para*-position to the coordinating N-atoms are known to have a stronger effect on the electron density at the metal center than substituents in *ortho*-position.[11a-c] Compared to the Ru(II) complex with 4,4',5,5'-tetramethylated bpy (Me_4bpy),[18] metal oxidation in $[Ru((MeO)_4bpy)_3]^{2+}$ is easier by about 0.2 V. The very electron-rich 4,4'-bis(dimethylamino)-substituted bpy ligand (4,4'-$(Me_2N)_2$bpy) on the other hand leads to an oxidation potential which is roughly 0.5 V lower than that of $[Ru((MeO)_4bpy)_3]^{2+}$.[20] However, the new $[Ru((MeO)_4bpy)_3]^{2+}$ and $[Os((MeO)_4bpy)_3]^{2+}$ complexes seem to be chemically significantly more robust than the $Ru(4,4'\text{-}(Me_2N)_2bpy)_3^{2+}$ complex.

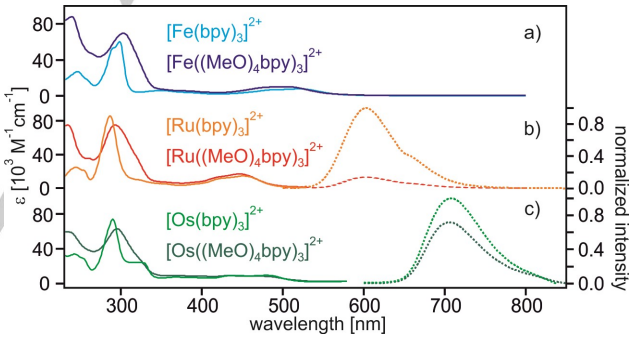

Figure 4. Optical absorption (solid lines) and luminescence spectra (dotted lines) of the $[M((MeO)_4bpy)_3]^{2+}$ and $[M(bpy)_3]^{2+}$ complexes in aerated CH_3CN at 22 °C. Excitation occurred at 455 nm for all complexes. The luminescence intensities were normalized to the luminescence emitted by the $[Ru(bpy)_3]^{2+}$ and $[Os(bpy)_3]^{2+}$ parent complexes, taking into account differences in absorbance at the excitation wavelength.

UV-Vis absorption and photoluminescence. The solid lines in Figure 4 are the optical absorption spectra of the $[M((MeO)_4bpy)_3]^{2+}$ complexes and $[M(bpy)_3]^{2+}$ reference compounds in CH_3CN at 22 °C. The lowest-energy absorption bands which are observable on this extinction scale are due to MLCT transitions in all 6 cases. For a given metal, the MLCT energy is similar in $[M((MeO)_4bpy)_3]^{2+}$ and $[M(bpy)_3]^{2+}$ complexes. This makes sense because metal oxidation was found to be roughly 0.4 V easier in the complexes with $(MeO)_4$bpy but at the same time ligand reduction was about 0.3 V more difficult than in

the bpy complexes. The ligand-based π-π* absorptions of $(MeO)_4$bpy near 300 nm are broadened with respect to those of ordinary bpy.

The dotted lines in Figure 4 are luminescence spectra recorded after excitation of the Ru(II) and Os(II) complexes in aerated CH_3CN at 455 nm. The Fe(II) complexes are non-emissive due to energetically low-lying d-d excited states. For the Ru(II) and Os(II) complexes the intensity has been normalized to that of the respective $[M(bpy)_3]^{2+}$ reference compounds in order to visualize the relative photoluminescence intensities of the new $[M((MeO)_4bpy)_3]^{2+}$ complexes and the known parent compounds. In the last column of Table 2 the luminescence quantum yields of the various complexes in aerated CH_3CN are reported. These quantum yields were estimated on the basis of the measured relative emission intensities and the known luminescence quantum yield for $[Ru(bpy)_3]^{2+}$ under identical conditions (Figure S11).[22] The $[M((MeO)_4bpy)_3]^{2+}$ complexes exhibit weaker luminescence than the $[M(bpy)_3]^{2+}$ parent compounds, possibly because of additional multiphonon relaxation pathways that come into play with molecular vibrations involving the methoxy-substituents.

Table 2. Lifetimes (τ_0) of the lowest-energetic ^{3}MLCT excited states and luminescence quantum yields (ϕ) in CH_3CN at 22 °C.

complex	$\tau_{0,\ aerated}$ [ns]	$\tau_{0,\ deaerated}$ [ns]	$\phi_{,\ aerated}$
$[Ru(bpy)_3]^{2+}$	173	830[a]	0.018[b]
$[Ru((MeO)_4bpy)_3]^{2+}$	33	57	0.002[c]
$[Os(bpy)_3]^{2+}$	42	56[d]	0.010[c]
$[Os((MeO)_4bpy)_3]^{2+}$	35	73	0.006[c]

[a] From ref. [23]. [b] From ref. [22]. [c] Determined from luminescence intensity measurements relative to $Ru(bpy)_3^{2+}$, corrected for differences in absorbance at excitation wavelengths. [d] From ref. [23a].

Luminescence lifetimes (τ_0) measured after excitation at 532 nm with laser pulses of ~10 ns duration were detected at 600 nm for the Ru(II) complexes and at 700 nm for the Os(II) complexes (Figure S12). The lifetimes in aerated and de-oxygenated CH_3CN at 22 °C are reported in Table 2. The luminescence lifetime of $[Ru((MeO)_4bpy)_3]^{2+}$ is roughly a factor of 5 shorter than that of $[Ru(bpy)_3]^{2+}$ in aerated CH_3CN whereas the luminescence quantum yields differ by a factor of 9 under identical conditions. This suggests that the radiative ^{3}MLCT decay rate constants differ by a factor 2 between these two complexes. For the two Os(II) complexes the correlation between luminescence quantum yield and luminescence lifetime is closer than in the case of the Ru(II) complexes, indicating that the radiative ^{3}MLCT decay rate constants are very similar for $[Os((MeO)_4bpy)_3]^{2+}$ and $[Os(bpy)_3]^{2+}$. The change from aerated to de-oxygenated CH_3CN is associated with significant increases in luminescence lifetimes due to the suppression of ^{3}MLCT relaxation via energy transfer to O_2 (third column of Table 2). However, even under these conditions the ^{3}MLCT lifetimes of $[Ru((MeO)_4bpy)_3]^{2+}$ and $[Os((MeO)_4bpy)_3]^{2+}$ stay well below 100 ns, which is significantly shorter than what is measured for $[Ru(bpy)_3]^{2+}$ under identical conditions.

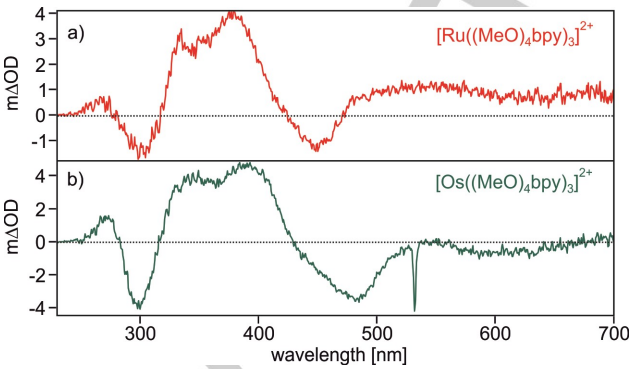

Figure 5. Transient difference spectra for ^{3}MLCT-excited $[Ru((MeO)_4bpy)_3]^{2+}$ and $[Os((MeO)_4bpy)_3]^{2+}$ in aerated CH_3CN at 22 °C. Excitation occurred with laser pulses of ~10 ns duration at 532 nm. The spectra were time-integrated over 200 ns. Sample concentrations were $1.4 \cdot 10^{-5}$ M and $0.9 \cdot 10^{-5}$ M for Ru(II) and Os(II), respectively.

Transient absorption spectroscopy. The $[Ru((MeO)_4bpy)_3]^{2+}$ and $[Os((MeO)_4bpy)_3]^{2+}$ complexes in aerated CH_3CN were excited at 532 nm with laser pulses of ~10 ns duration, and transient differences in optical absorption were probed with the white-light output of a high-pressure Xe lamp. Time-integration over the first 200 ns after the excitation pulses afforded the transient difference spectra shown in Figure 5. The two spectra are rather similar to one another because the same type of ^{3}MLCT excited state is probed in both cases. The most important difference is a red-shift of the MLCT bleach when going from the Ru(II) to the Os(II) complex due to the lower MLCT energy of the latter. Both spectra from Figure 5 are similar to the transient difference spectrum of the $[Ru(bpy)_3]^{2+}$ parent complex,[24] with a bleach around 300 nm caused by (partial) disappearance of π-π* absorption from neutral $(MeO)_4$bpy and an increase in absorbance between 320 and 430 nm caused by reduced $(MeO)_4$bpy. The negative signal at 600 nm in Figure 5b is an artifact.

The decays of the transient absorption signals of the $[Ru((MeO)_4bpy)_3]^{2+}$ complex at 300, 380, and 448 nm are within experimental accuracy the same as the decay of the ^{3}MLCT luminescence detected at 600 nm (Figure S13a), indicating that one is indeed probing the same excited state in transient absorption and photoluminescence experiments. This is also the case for the $[Os((MeO)_4bpy)_3]^{2+}$ complex (Figure S13b).

Photoredox properties. Having established that $[Ru((MeO)_4bpy)_3]^{2+}$ and $[Os((MeO)_4bpy)_3]^{2+}$ exhibit similar ^{3}MLCT excited states structures (Figure 5), similar ^{3}MLCT energies (Figure 4) but significantly lower ground-state oxidation potentials (Figure 3, Table 1) than the $[Ru(bpy)_3]^{2+}$ and $[Os(bpy)_3]^{2+}$ parent complexes, we were curious to check whether the new methoxylated complexes are indeed better

photoreductants than the parent compounds. In order to test this hypothesis, luminescence quenching experiments with $[Ru((MeO)_4bpy)_3]^{2+}$ and 1-chloro-4-nitrobenzene were performed. The latter exhibits an electrochemical potential for one-electron reduction of -1.44 V vs. Fc^+/Fc and therefore is a comparatively weak electron acceptor.[25] 1-chloro-4-nitrobenzene has been reported to quench the ^{3}MLCT excited state of $[Ru(bpy)_3]^{2+}$ very inefficiently with a rate constant for bimolecular electron transfer of $8.0 \cdot 10^6$ M^{-1} s^{-1} in CH_3CN at 22 °C,[26] and we were able to reproduce this number. When performing the same experiment with $[Ru((MeO)_4bpy)_3]^{2+}$ the luminescence data in Figure 6a/b were obtained. The gradual increase in 1-chloro-4-nitrobenzene concentration between 0 and 10 mM clearly induces significant luminescence quenching both with regard to luminescence intensity (Figure 6a) and luminescence lifetime (Figure 6b).

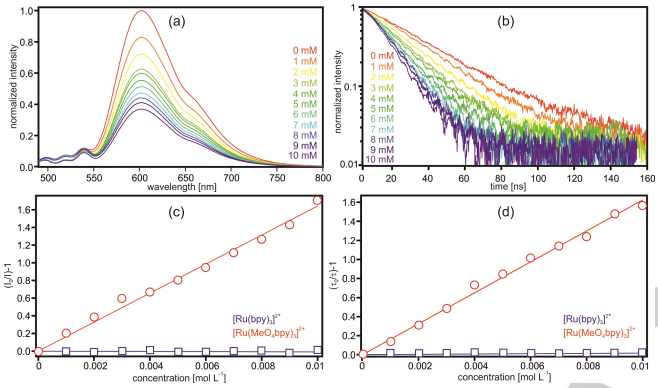

Figure 6. (a) Luminescence spectra of a $6.7 \cdot 10^{-6}$ M solution of $[Ru((MeO)_4bpy)_3]^{2+}$ in aerated CH_3CN as a function of increasing concentrations of 1-chloro-4-nitrobenzene (see inset). Excitation occurred at 455 nm, i. e., at a wavelength at which 1-chloro-4-nitrobenzene does not absorb significantly in the relevant concentration range. (b) Luminescence decays detected at 610 nm after excitation of the same solutions at 532 nm with laser pulses of ~10 ns duration. (c) Stern-Volmer plot based on the steady-state luminescence data from (a) (red circles); analogous data for the $[Ru(bpy)_3]^{2+}$ reference complex is also included (purple squares) (luminescence spectra not shown). (d) Stern-Volmer plot based on the decay data from (b) (red circles); analogous data for the $[Ru(bpy)_3]^{2+}$ reference complex is also included (purple squares) (luminescence decays not shown).

Based on the two sets of data in Figure 6a/b the Stern-Volmer plots shown in Figure 6c/d were established (red circles). Analogous data for the $[Ru(bpy)_3]^{2+}$ reference complex were also included (purple squares). The similarity of the Stern-Volmer plots for intensity and lifetime data for a given complex indicates that the excited state quenching is dynamic. From the slopes of linear regression fits to the data in Figure 6c/d and taking into account the ^{3}MLCT lifetimes of the $[Ru((MeO)_4bpy)_3]^{2+}$ and $[Ru(bpy)_3]^{2+}$ complexes, one obtains the rate constants (k_q) for oxidative excited state quenching reported in Table 3. For $[Ru((MeO)_4bpy)_3]^{2+}$ we found $k_q = 4.8 \cdot 10^9$ M^{-1} s^{-1}, i. e., a value which is a factor of 600 higher than what is found for $[Ru(bpy)_3]^{2+}$. For the parent complex, similarly rapid bimolecular quenching with nitroaromatic compounds was only observed for substances which have roughly 0.3 V more oxidative power.[25-26]

Table 3. Rate constants (k_q) for oxidative ^{3}MLCT excited state quenching by 1-chloro-4-nitrobenzene in aerated CH_3CN at 22 °C.

complex	k_q [M^{-1} s^{-1}]
$[Ru(bpy)_3]^{2+}$	$8.0 \cdot 10^6$ [a]
$[Ru((MeO)_4bpy)_3]^{2+}$	$4.8 \cdot 10^9$ [b]

[a] From ref. [26]. [b] This work (Figure 6).

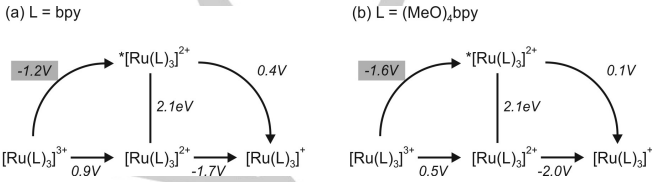

Figure 7. Latimer diagrams for $[Ru(bpy)_3]^{2+}$ and $[Ru((MeO)_4bpy)_3]^{2+}$. The asterisks mark the ^{3}MLCT-excited species. Potentials are for CH_3CN solution in V vs. Fc^+/Fc.

In Figure 7a the known Latimer diagram for $[Ru(bpy)_3]^{2+}$ is shown.[25] The Latimer diagram for $[Ru((MeO)_4bpy)_3]^{2+}$ established on the basis of our new data is shown in Figure 7b. The electrochemical potentials for one-electron reduction and oxidation in the electronic ground state were taken from Table 2 (Figure 3), and the ^{3}MLCT excited state energy was estimated to be identical as in $[Ru(bpy)_3]^{2+}$ (Figure 7b). This approximation makes sense because the ^{1}MLCT absorption bands are detected at similar wavelengths in $[Ru((MeO)_4bpy)_3]^{2+}$ and $[Ru(bpy)_3]^{2+}$ (Figure 4). Moreover we found that metal oxidation is about 0.4 V more favorable for the new methoxylated complexes but reduction of their ligands is roughly 0.3 V less favorable (Table 2). Thus, we assume that the error in ^{3}MLCT energy estimated in this manner is on the order of ±0.1 V. Figure 7 illustrates that ^{3}MLCT-excited $[Ru((MeO)_4bpy)_3]^{2+}$ is indeed a significantly better photoreductant with a potential of -1.6 V vs. Fc^+/Fc for oxidation in the ^{3}MLCT excited state compared to -1.2 V vs. Fc^+/Fc for $[Ru(bpy)_3]^{2+}$. This explains why 1-chloro-4-nitrobenzene with a reduction potential of -1.44 V vs. Fc^+/Fc reacts efficiently with ^{3}MLCT-excited $[Ru((MeO)_4bpy)_3]^{2+}$.

As far as the osmium complexes are concerned, the $[Os((MeO)_4bpy)_3]^{2+}$ compound is a stronger photoreductant than the $[Os(bpy)_3]^{2+}$ parent complex, too, because metal oxidation is significantly facilitated by the electron-donating methoxy-substituents. The ^{3}MLCT energy in this case is only ~1.8 eV, hence we estimate a potential of -1.7 V vs. Fc^+/Fc for oxidation in the long-lived ^{3}MLCT excited state of $[Os((MeO)_4bpy)_3]^{2+}$. Thus, photoexcited $[Ru((MeO)_4bpy)_3]^{2+}$ and $[Os((MeO)_4bpy)_3]^{2+}$ are both relatively potent photoreductants, as the comparison with other metal complexes in Table 4 shows. In order to put our results into somewhat greater perspective, Table 4 includes the excited-state oxidation potentials of some of the most potent photoreductants known to date.

Table 4. Electrochemical potentials for one-electron oxidation of selected metal complexes in their long-lived excited states (in V vs. Fc^+/Fc).

complex	E^0 (M^+/M^*)
$[Ru(bpy)_3]^{2+}$	-1.2 [a]
$[Ru((MeO)_4bpy)_3]^{2+}$	-1.6 [b]
$[Os(bpy)_3]^{2+}$	-1.4 [c]
$[Os((MeO)_4bpy)_3]^{2+}$	-1.7 [b]
$W(CNAr)_6$	< -2.7 [d]
$[Ir(\mu\text{-pz})(COD)]_2$	-2.2 [e]

[a] From ref. [26]. [b] This work. [c] Estimated on the basis of the ground-state oxidation potential reported in ref. [11a] and the ^{3}MLCT energy reported in ref. [27]. [d] From ref. [28] (CNAr = arylisocyanides). [e] From ref. [29] (μ-pz = μ-pyrazolyl; COD = 1,5-cyclooctadiene).

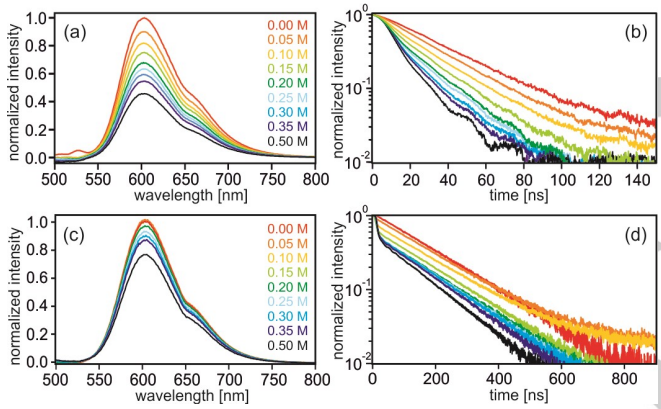

Figure 8. Luminescence of $[Ru((MeO)_4bpy)_3]^{2+}$ and $[Ru(bpy)_3]^{2+}$ in aerated CH_3CN at 22 °C in presence of 0.5 M acetophenone and increasing amounts of methanesulfonic acid (see insets). Excitation for the steady-state experiments (a, c) occurred at 455 nm. In the time-resolved experiments, excitation occurred at 532 nm with laser pulses of ~10 ns duration, and detection was at 610 nm. Data for $[Ru((MeO)_4bpy)_3]^{2+}$ (conc. $1.15\cdot10^{-5}$ M) are in panels a and b; data for $[Ru(bpy)_3]^{2+}$ (conc. $0.85\cdot10^{-5}$ M) are in panels c and d.

Proton coupled electron transfer. Evidently, the $[Ru((MeO)_4bpy)_3]^{2+}$ complex is a strong reductant in its ^{3}MLCT excited state, yet the previously explored $[Ru(4,4'\text{-}(Me_2N)_2bpy)_3]^{2+}$ complex is an even stronger (photo-)reductant (Table 1).[20] However, unlike the 4,4'-bis(dimethylamino)-substituted bpy ligands of the latter, the 4,4',5,5'-tetramethoxy-2,2'-bipyridine ligands of $[Ru((MeO)_4bpy)_3]^{2+}$ are not easily protonatable, and therefore this complex continues to exhibit its photoredox activity in acidic solution. This property is of interest for photoinduced PCET chemistry in which a substrate is reduced by the photoexcited $[Ru((MeO)_4bpy)_3]^{2+}$ complex and protonated by an acid which is simultaneously present. Ketones are particularly interesting substrates in this context because they are not easily reduced unless electron transfer is coupled to proton transfer to yield neutral ketyl radicals.[30] Recent studies reported on ketyl-olefin cyclization enabled by PCET, and this method proved to be of interest for organic synthesis.[31] The PCET reaction occurred between photogenerated $[Ru(bpy)_3]^+$, a series of Brönsted acids, and a variety of ketones. The ^{3}MLCT excited state of $[Ru(bpy)_3]^{2+}$ was unable to engage directly in PCET chemistry because it is not reducing enough, and therefore $[Ru(bpy)_3]^+$ had to be photogenerated by reductive ^{3}MLCT excited-state quenching with a Hantzsch dihydropyridine. Against this background we explored whether the ^{3}MLCT excited state of $[Ru((MeO)_4bpy)_3]^{2+}$ in acidic media could directly engage in PCET chemistry with ketones, without the use of Hantzsch dihydropyridine or other sacrificial electron donors.

Acetophenone was used as a model ketone for the subsequent PCET studies, and methanesulfonic acid was employed as a proton source. In pure CH_3CN without acid, acetophenone is unable to quench the ^{3}MLCT excited state of $[Ru((MeO)_4bpy)_3]^{2+}$ because electron transfer and (triplet-triplet) energy transfer processes are energetically unfavorable. The reduction potential of acetophenone in CH_3CN is -2.48 V vs. Fc^+/Fc,[32] and its triplet energy is 3.21 eV;[33] the excited-state oxidation potential of $[Ru((MeO)_4bpy)_3]^{2+}$ in CH_3CN is -1.6 V vs. Fc^+/Fc and the ^{3}MLCT energy is 2.1 eV (see above). Consequently, electron transfer and triplet-triplet energy transfer are both endergonic by more than 0.8 eV. However, upon addition of increasing amounts of methanesulfonic acid to an aerated CH_3CN solution containing $1.15\cdot10^{-5}$ M $[Ru((MeO)_4bpy)_3]^{2+}$ and 0.5 M acetophenone, increasingly strong luminescence quenching is observed (Figure 8). Addition of 0.5 M methanesulfonic acid leads to a decrease in the luminescence intensity by roughly 50% (Figure 8a), and this is accompanied by a decrease in ^{3}MLCT luminescence lifetime from 35 ns in absence of acid to 11 ns in presence of 0.5 M methanesulfonic acid (Figure 8b). When performing the exact same experiment with the $[Ru(bpy)_3]^{2+}$ reference complex, the luminescence intensity decreases only by ~20% (Figure 8c), and the lifetime shortens only from 173 ns to 133 ns (Figure 8d). In the lifetime data from Figure 8d instrumentally limited decay components become visible; these are due to a fluorescence which is observed as soon as methanesulfonic acid is added to 0.5 M acetophenone in CH_3CN (Figure S14). In the luminescence spectra of Figure 8a/c the respective (comparatively weak) fluorescence signal has been subtracted as described in the supporting information. Control experiments in which 0.5 M methanesulfonic acid has been added to aerated CH_3CN solutions containing $[Ru((MeO)_4bpy)_3]^{2+}$ or $[Ru(bpy)_3]^{2+}$ but no acetophenone did not reveal any significant luminescence quenching (data not shown). Thus it is clear that acetophenone and methanesulfonic acid must be simultaneously present in order to induce excited-state quenching.

Direct observation of the ketyl radical of acetophenone by transient absorption spectroscopy is complicated by the fact that in the visible portion of the spectrum this particular ketyl exhibits only two comparatively weak absorption bands, the first one with

a maximum at ~405 nm and the second at ~440 nm, both with extinction coefficients of ~2000 M^{-1} cm^{-1}. [34] In the UV there are stronger ketyl absorptions, but detection in this range is hampered by the large excess of absorbing acetophenone present in solution. Nonetheless, the transient absorption spectrum shown in Figure S15 is compatible with the formation of ketyl, albeit the spectrum is dominated by the more intense spectral features of the oxidized ruthenium complex (see supporting information for further details).

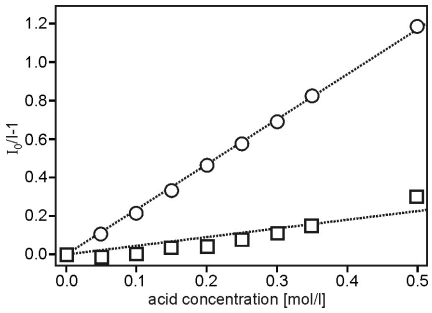

Figure 9. Stern-Volmer plot based on the luminescence intensity data from Figure 8a/c, measured for $[Ru((MeO)_4bpy)_3]^{2+}$ (circles) and $[Ru(bpy)_3]^{2+}$ (squares) in aerated CH_3CN at 22 °C in presence of 0.5 M acetophenone and increasing amounts of methanesulfonic acid.

Figure 9 shows a Stern-Volmer plot based on the luminescence intensity data from Figure 8a/c. Using ^{3}MLCT lifetimes (τ_0) of 33 ns and 173 ns in aerated CH_3CN (Table 2), excited-state quenching constants ($k_{q,acid}$) of $(6.6\pm0.1)\cdot10^7$ M^{-1} s^{-1} and $(2.6\pm0.3)\cdot10^6$ M^{-1} s^{-1} are extracted for $[Ru((MeO)_4bpy)_3]^{2+}$ and $[Ru(bpy)_3]^{2+}$, respectively (Table 5). More quantitatively correct models would take the hydrogen-bonding equilibrium between methanesulfonic acid and acetophenone in CH_3CN into account,[30, 35] but the currently available data do not permit this treatment (see supporting information on page S13 for further details). Note that acetophenone is only a very weak base in CH_3CN (pK_a = -0.1)[31a] which is not easily protonated even by methanesulfonic acid (pK_a = 10.0).[36] Based on these pK_a values, at the highest concentration of methanesulfonic acid used in Figure 9 (0.5 M acid in presence of 0.5 M of acetophenone), the concentration of protonated acetophenone is only $5\cdot10^{-6}$ M.

Table 5. Rate constants ($k_{q,acid}$) for ^{3}MLCT excited state quenching by methanesulfonic acid in CH_3CN at 22 °C in presence of 0.5 M acetophenone; formal bond dissociation free energies (*f*BDFEs) for the reaction couples comprised of photoexcited Ru(II) complex and methanesulfonic acid in CH_3CN (see text for details).

complex	$k_{q,acid}$ [M^{-1} s^{-1}]	*f*BDFE [kcal/mol]
$[Ru(bpy)_3]^{2+}$	$(2.6\pm0.3)\cdot10^6$	40.9
$[Ru((MeO)_4bpy)_3]^{2+}$	$(6.6\pm0.1)\cdot10^7$	31.6

The hydrogen-bonding equilibrium between methanesulfonic acid and acetophenone is largely independent of which one of the two ruthenium(II) complexes is present, particularly because the concentrations of the latter are only in the micromolar range. Consequently, in both experiments from Figure 9 essentially identical concentrations of hydrogen-bonded acetophenone / methanesulfonic acid couples are present at the individual acid concentrations, and we conclude from the data in Table 5 that the ^{3}MLCT excited state of $[Ru((MeO)_4bpy)_3]^{2+}$ reacts with acetophenone in acidic CH_3CN roughly 25 times more rapidly than the ^{3}MLCT excited state of $[Ru(bpy)_3]^{2+}$. This is attributed to the stronger reducing power of the $[Ru((MeO)_4bpy)_3]^{2+}$ complex. However, the reduction must evidently occur in proton-coupled fashion, and the driving-force for the overall PCET process is a function not just of reducing power but also of acid strength.[37] For the $[Ru((MeO)_4bpy)_3]^{2+}$ / methanesulfonic acid reaction couple in CH_3CN one can estimate a formal bond dissociation free energy (*f*BDFE) according to equation 1.[37a, 38] In this equation, pK_a is the acidity constant of the acid in CH_3CN, E^0 is the standard oxidation potential of the electron donor (in V vs. Fc^+/Fc in CH_3CN), and the $C_{G,sol}$ term describes the free energies for formation and solvation of H· (in CH_3CN).

$$f\text{BDFE [kcal/mol]} = 1.37\cdot pK_a + 23.06\cdot E^0 + C_{G,sol} \quad \text{(eq. 1)}$$

The *f*BDFE is a measure of the energetic cost associated with the coupled oxidation of ^{3}MLCT-excited $[Ru((MeO)_4bpy)_3]^{2+}$ and the deprotonation of methanesulfonic acid. The *f*BDFE relies on the fact that even though electron and proton may come from different sources, the overall PCET thermochemistry is equivalent to a reaction in which there is a single hydrogen-atom source (donating both an electron and a proton). Using pK_a = 10.0,[36] E^0 = -1.6 V vs. Fc^+/Fc (Figure 7), and $C_{G,sol}$ = 54.9 kcal/mol,[37a, 38] one obtains *f*BDFE = 31.6 kcal/mol for the reaction couple consisting of ^{3}MLCT-excited $[Ru((MeO)_4bpy)_3]^{2+}$ and methanesulfonic acid in CH_3CN. For the O-H bond in the ketyl radical of acetophenone, a BDFE of 26 kcal/mol has been reported.[31] Using this value, we estimate that termolecular PCET involving photoexcited $[Ru((MeO)_4bpy)_3]^{2+}$, methanesulfonic acid, and acetophenone is endergonic by 5.6 kcal/mol. The analogous PCET reaction involving photoexcited $[Ru(bpy)_3]^{2+}$ (E^0 = -1.2 V vs. Fc^+/Fc) is estimated to be endergonic by 14.9 kcal/mol (*f*BDFE = 40.9 kcal/mol, Table 5). Both of these estimates are associated with uncertainties on the order of 2-3 kcal/mol, yet it is clear that there is a significant difference in PCET driving forces between the $[Ru((MeO)_4bpy)_3]^{2+}$ and $Ru(bpy)_3^{2+}$ systems. This interpretation is compatible with the observed reaction kinetics (Table 5).

Concerted proton-electron transfer (CPET) is likely to be the prevalent reaction mechanism in the phototriggered reaction between $[Ru((MeO)_4bpy)_3]^{2+}$, acetophenone, and methanesulfonic acid (Scheme 2). A mechanism with consecutive electron and proton transfer steps (ET-PT) can be excluded on the basis of the unfavorable reaction free energy for the initial electron transfer event (ΔG_{ET}^0 = 0.9 eV based on the potentials reported above); the lack of any significant $[Ru((MeO)_4bpy)_3]^{2+}$ luminescence quenching even in presence

of 0.5 M acetophenone (in absence of acid) strongly supports this argument. A stepwise proton transfer, electron transfer (PT-ET) sequence with a proton transfer pre-equilibrium preceding a fast electron transfer step is unlikely because the concentration of protonated acetophenone is very small. As noted above, even in presence of 0.5 M acetophenone and 0.5 M methanesulfonic acid, the concentration of protonated acetophenone is only $5 \cdot 10^{-6}$ M. This leaves us with concerted proton-electron transfer as the most plausible mechanism for PCET in this case.

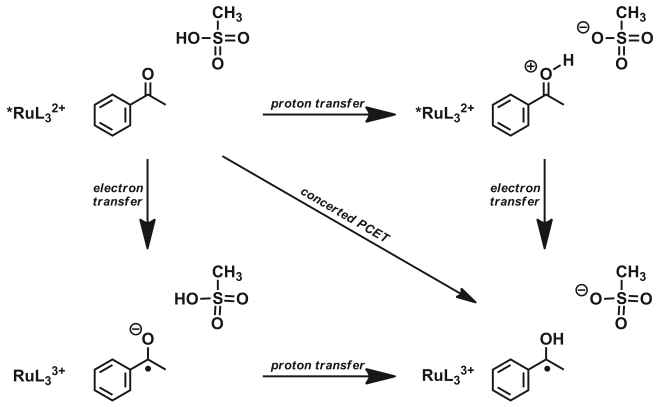

Scheme 2. Mechanistic pathways for PCET. L = MeO_4bpy. The asterisk denotes the photoexcited complex.

Conclusions

4,4',5,5'-Tetramethoxy-2,2'-bipyridine ($(MeO)_4$bpy) had been reported in the literature only once as part of a broad (organic) synthetic study of pyridines,[12] but to our knowledge it had never been used as a ligand to any metal until now. We developed a new synthetic procedure to make $(MeO)_4$bpy in 6 steps from commercial 2-chloro-5-hydroxypyridine. The presence of twelve electron-donating methoxy-substituents on homoleptic Fe(II), Ru(II), and Os(II) complexes with $(MeO)_4$bpy makes these complexes very strong electron donors. Both the $[Ru((MeO)_4bpy)_3]^{2+}$ and the $[Os((MeO)_4bpy)_3]^{2+}$ complex are significantly stronger excited-state electron donors than the $[Ru(bpy)_3]^{2+}$ and $[Os(bpy)_3]^{2+}$ parent compounds. As an example, ^{3}MLCT-excited $[Ru((MeO)_4bpy)_3]^{2+}$ is able to reduce even relatively mild oxidants such as 1-chloro-4-nitrobenzene. Even in presence of strong acids such as methanesulfonic acid (pKa = 10.0 in CH_3CN),[36] the $[Ru((MeO)_4bpy)_3]^{2+}$ complex is stable in CH_3CN solution for several hours and remains un-protonated. As a consequence, $[Ru((MeO)_4bpy)_3]^{2+}$ can engage in proton-coupled electron transfer (PCET) chemistry with ketones to form (neutral) ketyl radicals directly from the ^{3}MLCT excited state, as demonstrated on the specific example of acetophenone. Analogous PCET chemistry with the $[Ru(bpy)_3]^{2+}$ parent complex is significantly less efficient. The two main disadvantages of $[Ru((MeO)_4bpy)_3]^{2+}$ with respect to the $Ru(bpy)_3^{2+}$ complex are its comparatively short ^{3}MLCT lifetime (35 ns vs. 173 ns in aerated CH_3CN), and the fact that 4,4',5,5'-tetramethoxy-2,2'-bipyridine has to be synthesized in 6 steps while the bpy parent ligand is commercially available. Nevertheless our study demonstrates that $[Ru((MeO)_4bpy)_3]^{2+}$ clearly outperforms the ordinary $[Ru(bpy)_3]^{2+}$ complex as a photoreductant, both in neutral and acidic CH_3CN.

Experimental Section

The yields reported in the following are average values of at least two attempts. All commercial compounds were used as received. The only exception is zinc powder which was activated as described previously.[17a]

2-Chloro-5-hydroxypyridine (**2**). The following procedure was developed based on a previously published protocol.[14] To an ice-cooled solution of commercial 2-chloro-5-aminopyridine (**1**) (5 g, 38.8 mmol, 1 eq.) in sulfuric acid (50 wt. %, 74 ml) was added 5 ml of an aqueous solution of $NaNO_2$ (3.22 g, 46.6 mmol, 1.2 eq.) in such a manner that the temperature of the reaction mixture did not exceed 5 °C. After stirring at room temperature for 30 minutes, the mixture was added to concentrated acetic acid (100 ml) at 100 °C. Stirring was continued at this temperature overnight. Then the cooled reaction mixture was neutralized with saturated aqueous Na_2CO_3 solution and extracted with ethyl acetate (5 × 200 ml). The combined organic phases were dried over anhydrous Na_2SO_4 and evaporated. The resulting orange solid was purified by column chromatography on silica gel using a 4:1 (v:v) mixture of pentane and ethyl acetate as the eluent. The pure product was obtained in the form of colorless needles (54% yield). ^{1}H NMR (400 MHz, acetone-d_6): δ [ppm] 9.01 (s, 1 H), 7.98 (dd, *J* = 2.9, 0.8 Hz, 1 H), 7.29 (dd, *J* = 8.6, 2.9 Hz, 1 H), 7.26 (dd, *J* = 8.6, 0.8 Hz, 1 H). ^{13}C NMR (101 MHz, acetone-d_6): δ [ppm] 154.2, 141.8, 138.3, 126.9, 125.4. ESI-MS: 128.0. Elemental analysis: found C, 46.68; H, 3.33; N, 11.19; calc. for C_5H_4NOCl: C, 46.36; H, 3.11; N, 10.81.

2-Chloro-5-methoxypyridine (**3**). 2-Cloro-5-hydroxypyridine (**2**) (1 eq.) was dissolved in dry acetonitrile (3 ml per mmol of **2**) and stirred with K_2CO_3 (1.5 eq.) at room temperature for 15 minutes. Iodomethane (1.05 eq.) was added to the orange solution. The reaction mixture turned dark yellow and stirring was continued overnight. Then the solvent was removed on a rotary evaporator, and the residue was vigorously stirred in a mixture of water and diethyl ether for 5 minutes. The aqueous and organic phases were separated, and the aqueous phase was extracted twice with diethyl ether. The combined ether phases were washed with brine and dried over anhydrous Na_2SO_4. After solvent evaporation the pure product was obtained as an orange-yellow liquid (63% yield). ^{1}H NMR (400 MHz, $CDCl_3$): δ [ppm] 8.06 (d, *J* = 2.9 Hz, 1 H), 7.23 (dd, *J* = 8.8, 0.7 Hz, 1 H), 7.18 (dd, *J* = 8.8, 2.9 Hz, 1 H), 3.85 (s, 3 H). ^{13} C NMR (101 MHz, $CDCl_3$) δ [ppm] 155.1, 142.7, 136.3, 124.6, 124.5, 56.1. ESI-MS: 144.0.

2-Chloro-5-methoxypyridine-*N*-oxide (**4**). The following procedure was adapted from a previously published protocol.[15] Urea·H_2O_2 adduct (2 eq.) was added in one portion to an ice-cooled solution of 2-chloro-5-methoxypyridine (**3**) (1 eq.) in dry dichloromethane (22 ml per mmol of **3**). Trifluoroacetic anhydride (1.8 eq.) was added dropwise. Then the reaction was allowed to reach room temperature and stirring was continued overnight. An aqueous solution of sodium thiosulfate was added carefully to the reaction mixture in order to destroy unreacted peroxide and vigorous stirring was continued for one hour. Then the phases were separated and the aqueous phase was extracted three times with dichloromethane. The combined organic phases were dried over anhydrous Na_2SO_4 and the solvent was removed on a rotary evaporator. The pure product was obtained as a white solid after column

chromatography on silica gel using a 75:1 (v:v) mixture of CH_2Cl_2 and CH_3OH as the eluent (69% yield). ^1H NMR (400 MHz, $CDCl_3$): δ [ppm] 8.13 (d, *J* = 2.6 Hz, 1 H), 7.36 (d, *J* = 9.1 Hz, 1 H), 6.88 (dd, *J* = 9.1, 2.6 Hz, 1 H), 3.84 (s, 3 H). ^{13}C NMR (101 MHz, $CDCl_3$): δ [ppm] 156.2, 133.9, 128.2, 126.0, 114.3, 56.3. ESI-MS: 160.0. Elemental analysis: found C, 44.95; H, 3.95; N, 8.95; calc. for $C_6H_6NO_2Cl$: C, 44.95; H, 3.79; N, 8.78.

2-Chloro-4-nitro-5-methoxypyridine (**5**). 2-Chloro-5-methoxypyridine-*N*-oxide (**4**) (1 eq.) was dissolved in concentrated sulfuric acid (1.1 ml per mmol of **4**), and concentrated (65%) nitric acid (0.55 ml per mmol of **4**) was added. The reaction mixture was heated to 100 °C overnight. After cooling to room temperature, the mixture was poured on ice, and then aqueous NaOH solution (40 wt. %) was added carefully to adjust the pH to 14. The resulting precipitate was dissolved in dichloromethane and the aqueous supernatant was extracted with dichloromethane four times (using 8.5 ml per mmol of **4**). The combined organic phases were dried over anhydrous Na_2SO_4, and then the solvent was removed on a rotary evaporator. The light yellow crude product was purified by column chromatography on silica gel using a 2:1 (v:v) mixture of pentane and ethyl acetate as the eluent. This afforded the pure product as a white solid (44% yield). ^1H NMR (400 MHz, $CDCl_3$): δ [ppm] 8.35 (s, 1 H), 7.66 (s, 1 H), 4.07 (s, 3 H). ^{13}C NMR (101 MHz, $CDCl_3$): δ [ppm] 146.6, 145.9, 143.1, 137.0, 118.5, 57.7. Elemental analysis: found C, 38.41; H, 2.79; N, 14.50; calc. for $C_6H_5N_2O_3Cl$ C, 38.22; H, 2.67; N, 14.86.

2-Chloro-4,5-dimethoxypyridine (**6**). This compound was prepared following a method developed for related reactants.[16] 2-Chloro-4-nitro-5-methoxypyridine (**5**) (1 eq.) was dissolved in dry THF (1.4 ml per mmol of **5**) and $TBAOCH_3$ (20 wt. % in CH_3OH, 1 eq.) was added. The mixture was stirred at room temperature until no starting material was left (as verified by TLC) which was usually the case after 2-3 hours. Then the solvent was removed on a rotary evaporator. The crude product was purified by flash chromatography on silica gel using diethyl ether as the eluent. This afforded the pure product as a white solid (89% yield). ^1H NMR (400 MHz, $CDCl_3$): δ [ppm] 7.73 (s, 1 H), 6.69 (s, 1 H), 3.81 (s, 2×3 H). ^{13}C NMR (101 MHz, $CDCl_3$): δ [ppm] 156.7, 145.3, 143.9, 131.7, 106.7, 56.6, 56.1. ESI-MS: 174.0. Elemental analysis: found C, 48.67; H, 4.87; N, 8.03; calc. for $C_7H_8NO_2Cl$: C, 48.43; H, 4.64; N, 8.07.

4,4',5,5'-Tetramethoxy-2,2'-bipyridine (**7**, $(MeO)_4$bpy). This ligand was prepared following a general procedure for the homocoupling of pyridines.[17] In our hands, the use of excess triphenylphosphine as described earlier proved to be problematic because of difficulties in the process of product purification.[12] $Ni(PPh_3)_2Cl_2$ (0.2 eq.), activated Zn powder (1.7 eq.) and Et_4NI (1 eq.) were stirred at room temperature in dry THF (4 ml per mmol of Et_4NI) under inert atmosphere for 1 hour. The color of the solution turned from dark blue over greenish to dark red during this time. 2-Chloro-4,5-dimethoxypyridine (**6**) (1 eq.) was dissolved in dry THF (4 ml per mmol of **6**) and was then added to the dark red reaction mixture. The latter immediately turned brown. This mixture was stirred under inert atmosphere at 50 °C overnight. After cooling to room temperature, the reaction mixture was poured into a mixture of 2 M aqueous NH_3 solution (30 ml per mmol of **6**) and dichloromethane (50 ml per mmol of **6**), and stirring was continued for 30 minutes. The resulting grey precipitate was filtered off, and the phases were separated. The organic phase was dried over anhydrous Na_2SO_4 and the solvent was removed on a rotary evaporator. The solid residue was purified by column chromatography on silica gel using a 97:3 (v:v) mixture of ethyl acetate and methanol as the eluent. This procedure afforded ligand **7** as an off-white solid (66% yield). ^1H NMR (400 MHz, $CDCl_3$): δ [ppm] 8.11 (s, 2 H), 7.92 (s, 2 H), 4.00 (s, 6 H), 3.95 (s, 6 H). ^{13}C NMR (101 MHz, $CDCl_3$): δ [ppm] 155.8, 151.0, 145.9, 132.1, 103.4, 56.7, 56.0. HR ESI-MS: found 277.1188, calc. 277.1186. Elemental analysis: found C, 60.35; H, 5.95; N, 9.29; calc. for $C_{14}H_{16}N_2O$: (+0.25 EtOAc) C, 60.39; H, 6.08; N, 9.29.

$[Fe((MeO)_4bpy)](BF_4)_2$. Commercial $Fe(BF_4)_2{\cdot}6H_2O$ (1 eq.) was dissolved in a minimal amount of dry and de-oxygenated acetonitrile. A solution of ligand **7** ($(MeO)_4$bpy) (3 eq.) in a minimal amount of chloroform was added. The initially colorless iron solution turned dark red, and stirring at room temperature was continued for 20 minutes. Then the solvent was evaporated under reduced pressure and the residue was re-dissolved in acetonitrile. The product was crystallized from acetonitrile by diffusion of diethyl ether vapor (96% yield). For elemental analysis, the NMR sample was dried at 80 °C under reduced pressure over night. ^1H NMR (400 MHz, acetone-d_6): δ [ppm] 8.40 (s, 6 H), 6.99 (s, 6 H), 4.09 (s, 18 H), 3.59 (s, 18 H). ^{13}C NMR spectra could not be measured because the complex was unstable over the time required for acquisition of such spectra. HR ESI-MS: found 442.1341 (M^{2+}), calc. 442.1335. Elemental analysis: found C, 46.52; H, 5.18; N, 7.51; calc. for $C_{42}H_{48}N_6O_{12}F_{12}FeP_2$ + 2 CH_3CN + 3 CH_3COCH_3: C, 46.16; H, 5.07; N, 7.83.

$[Fe((MeO)_4bpy)_3](SO_3CF_3)_2$. This compound was prepared in analogous manner as the tetrafluoroborate salt but with $Fe(OTf)_2$ instead of $Fe(BF_4)_2{\cdot}6H_2O$ as a starting material. The triflate salt of $[Fe((MeO)_4bpy)]^{2+}$ was made in the course of crystallization attempts. Slow diffusion of diethyl ether vapor into an acetonitrile solution afforded crystals which were used to obtain the X-ray diffraction data shown in Figure 2.

$[Ru((MeO)_4bpy)](PF_6)_2$. $RuCl_3{\cdot}0.5\ H_2O$ (1eq.) and 4,4',5,5'-tetramethoxy-2,2'-bipyridine (**7**, $(MeO)_4$bpy) (3.5 eq.) were heated to 190 °C in ethylene glycol (2 ml) under inert atmosphere for 4 hours. The cooled orange solution was treated with several portions of diethyl ether until the product stuck to the walls of the flask. The solid residue was then solved in acetonitrile and added dropwise to diethyl ether. The resulting suspension was filtered, washed with diethyl ether, and the solid was re-dissolved in de-ionized water. Purification occurred by column chromatography on silica gel using a 100:10:1 (v:v:v) mixture of acetone, de-ionized water, and saturated aqueous KNO_3 as the eluent. Acetone was evaporated from the desired chromatography fractions, and the pure complex was precipitated as a hexafluorophosphate salt by adding saturated aqueous KPF_6 solution. The precipitate was solved in dichloromethane. After drying over anhydrous Na_2SO_4, the solvent was removed on a rotary evaporator. The product was obtained as a red solid (72% yield), which was re-dissolved in acetonitrile in order to transfer it to a smaller flask. Then the solvent was removed on a rotary evaporator. ^1H NMR (400 MHz, CD_3CN): δ [ppm] 7.84 (s, 6 H), 7.03 (s, 6 H), 4.08 (s, 18 H), 3.56 (s, 18 H). ^{13}C NMR (101 MHz, CD_3CN): δ [ppm] 157.2, 153.2, 148.6, 134.3, 107.7, 57.8, 57.3. HR ESI-MS: found 465.1194 (M^{2+}), calc. 465.1182. Elemental analysis: found C, 43.15; H, 4.52; N, 6.84; calc. for $C_{42}H_{48}N_6O_{12}F_{12}RuP_2$ + 0.5 CH_3CN + 1.5 CH_3COCH_3: C, 42.98; H, 4.44; N, 6.86.

$[Os((MeO)_4bpy)](PF_6)_2$. This compound was prepared in analogous manner as $[Ru((MeO)_4bpy)](PF_6)_2$ using $(NH_4)_2OsCl_6$ as a metal source instead of $RuCl_3{\cdot}0.5\ H_2O$. The product was obtained as a dark green to blackish solid (64% yield). ^1H NMR (400 MHz, CD_3OD): δ [ppm] 9.49 (s, 6 H), 8.49 (s, 6 H), 5.34 (s, 18 H), 4.86 (s, 18 H). ^{13}C NMR (101 MHz, CD_3OD): δ [ppm] 176.0, 174.6, 168.3, 127.1, 119.2, 76.5, 76.3. HR ESI-MS: found 510.1476 (M^{2+}), calc. 510.1467. Elemental analysis: found C, 40.09; H, 4.58; N, 6.20; calc. for $C_{42}H_{48}N_6O_{12}F_{12}OsP_2$ + 2 CH_3COCH_3: C, 40.45; H, 4.24; N, 5.90.

X-ray crystallography. The crystals were measured on a Bruker Kappa Apex2 diffractometer at 123 K using graphite-monochromated Cu K_α radiation with λ = 1.5418 Å. The Apex software was used for data

collection and integration.[39] The structures were solved by the charge flipping method using the program Superflip.[40] Least-squares refinement against F was carried out on all non-hydrogen atoms using the program CRYSTALS.[41] Plots were produced using MERCURY.[42] Crystallographic data (excluding structure factors) for the structures in this paper have been deposited with the Cambridge Structural Data Center, the deposition numbers are: CCDC 1037160, 1037161, 1037162, 1037163.

Methods and equipment. ^{1}H and ^{13}C NMR spectra were measured on a 400 MHz Bruker Avance III instrument. ^{1}H NMR spectra of all relevant compounds are shown in the supporting information (Figures S1-S9). High-resolution mass spectrometry was performed with a Bruker maxis 4G QTOF ESI spectrometer, low-resolution mass spectra were measured on a Bruker esquire 3000 plus instrument. Elemental analysis occurred with a Varia Micro Cube instrument from Elementar and was conducted by Ms. Sylvie Mittelheisser in the Department of Chemistry at University of Basel. A Cary 5000 UV-Vis-NIR spectrophotometer from Varian was employed for optical absorption spectroscopy, and a Fluorolog-322 instrument from Horiba Jobin-Yvon was used for steady-state luminescence spectroscopy. Time-resolved luminescence and transient absorption spectroscopy was performed with an LP920-KS spectrophotometer from Edinburgh Instruments using the frequency-doubled output of a Quantel Brilliant b laser for excitation and either a R928 photomultiplier tube or an iCCD camera from Andor for detection. The duration of the laser pulses was approximately 10 ns, the pulse frequency was 10 Hz. Transient absorption (difference) spectra were time-averaged over a duration of 200 ns. Quartz cuvettes from Starna were used for all optical spectroscopic studies. Cyclic voltammetry was performed in a conventional setup with three electrodes using a Versastat3-200 potentiostat from Princeton Applied Research. A glassy carbon disk served as a working electrode, and two silver wires were used as counter and quasi-reference electrodes, respectively. Internal potential calibration occurred by addition of small amounts of ferrocene. The measurements were performed in dry acetonitrile with 0.1 M tetrabutylammonium hexafluorophosphate ($TBAPF_6$) as supporting electrolyte.

Acknowledgements

This work was supported by the Swiss National Science Foundation through grant number 200021_156063/1. Support from COST action CM1202 PERSPECT-H2O is acknowledged.

Keywords: photochemistry • electron transfer • photocatalysis • time-resolved spectroscopy • proton-coupled electron transfer

[1] A. Juris, V. Balzani, F. Barigelletti, S. Campagna, P. Belser, A. Von Zelewsky, *Coord. Chem. Rev.* **1988**, *84*, 85-277.

[2] T. J. Meyer, *Pure Appl. Chem.* **1986**, *58*, 1193-1206.

[3] a) M. S. Lowry, S. Bernhard, *Chem. Eur. J.* **2006**, *12*, 7970-7977; b) K. S. Schanze, D. B. MacQueen, T. A. Perkins, L. A. Cabana, *Coord. Chem. Rev.* **1993**, *122*, 63-89; c) K. N. Swanick, S. Ladouceur, E. Zysman-Colman, Z. F. Ding, *Chem. Commun.* **2012**, *48*, 3179-3181; d) R. D. Costa, E. Orti, H. J. Bolink, F. Monti, G. Accorsi, N. Armaroli, *Angew. Chem. Int. Ed.* **2012**, *51*, 8178-8211.

[4] a) V. Balzani, A. Juris, M. Venturi, S. Campagna, S. Serroni, *Chem. Rev.* **1996**, *96*, 759-833; b) M. H. Keefe, K. D. Benkstein, J. T. Hupp, *Coord. Chem. Rev.* **2000**, *205*, 201-228; c) H. Yersin, A. F. Rausch, R. Czerwieniec, T. Hofbeck, T. Fischer, *Coord. Chem. Rev.* **2011**, *255*, 2622-2652; d) M. Cattaneo, F. Fagalde, C. D. Borsarelli, N. E. Katz, *Inorg. Chem.* **2009**, *48*, 3012-3017; e) A. Breivogel, M. Park, D. Lee, S. Klassen, A. Kuhnle, C. Lee, K. Char, K. Heinze, *Eur. J. Inorg. Chem.* **2014**, *2014*, 288-295.

[5] a) A. Hagfeldt, M. Grätzel, *Chem. Rev.* **1995**, *95*, 49-68; b) A. Hagfeldt, G. Boschloo, L. C. Sun, L. Kloo, H. Pettersson, *Chem. Rev.* **2010**, *110*, 6595-6663; c) R. Argazzi, C. A. Bignozzi, T. A. Heimer, F. N. Castellano, G. J. Meyer, *Inorg. Chem.* **1994**, *33*, 5741-5749.

[6] a) A. E. Friedman, J. C. Chambron, J. P. Sauvage, N. J. Turro, J. K. Barton, *J. Am. Chem. Soc.* **1990**, *112*, 4960-4962; b) K. E. Erkkila, D. T. Odom, J. K. Barton, *Chem. Rev.* **1999**, *99*, 2777-2795; c) Y. Sun, D. A. Lutterman, C. Turro, *Inorg. Chem.* **2008**, *47*, 6427-6434; d) E. Baggaley, M. R. Gill, N. H. Green, D. Turton, I. V. Sazanovich, S. W. Botchway, C. Smythe, J. W. Haycock, J. A. Weinstein, J. A. Thomas, *Angew. Chem. Int. Ed.* **2014**, *53*, 3367-3371.

[7] a) O. S. Wenger, *Coord. Chem. Rev.* **2009**, *253*, 1439-1457; b) S. Van Wallendael, D. P. Rillema, *Coord. Chem. Rev.* **1991**, *111*, 297-318; c) L. De Cola, P. Belser, *Coord. Chem. Rev.* **1998**, *177*, 301-346; d) A. I. Baba, J. R. Shaw, J. A. Simon, R. P. Thummel, R. H. Schmehl, *Coord. Chem. Rev.* **1998**, *171*, 43-59; e) A. Vlček, M. Busby, *Coord. Chem. Rev.* **2006**, *250*, 1755-1762.

[8] a) J. M. R. Narayanam, C. R. J. Stephenson, *Chem. Soc. Rev.* **2011**, *40*, 102-113; b) C. K. Prier, D. A. Rankic, D. W. C. MacMillan, *Chem. Rev.* **2013**, *113*, 5322-5363; c) C. D. Windle, R. N. Perutz, *Coord. Chem. Rev.* **2012**, *256*, 2562-2570; d) B. Kumar, M. Llorente, J. Froehlich, T. Dang, A. Sathrum, C. P. Kubiak, *Annu. Rev. Phys. Chem.* **2012**, *63*, 541-569; e) X. Sala, S. Maji, R. Bofill, J. Garcia-Anton, L. Escriche, A. Llobet, *Acc. Chem. Res.* **2014**, *47*, 504-516.

[9] M. Goez, C. Kerzig, R. Naumann, *Angew. Chem. Int. Ed.* **2014**, *53*, 9914-9916.

[10] a) O. S. Wenger, *Acc. Chem. Res.* **2011**, *44*, 25-35; b) O. S. Wenger, *Acc. Chem. Res.* **2013**, *46*, 1517-1526.

[11] a) A. B. P. Lever, *Inorg. Chem.* **1990**, *29*, 1271-1285; b) E. S. Dodsworth, A. B. P. Lever, *Chem. Phys. Lett.* **1986**, *124*, 152-158; c) A. B. P. Lever, *Inorg. Chem.* **1991**, *30*, 1980-1985; d) N. H. Damrauer, T. R. Boussie, M. Devenney, J. K. McCusker, *J. Am. Chem. Soc.* **1997**, *119*, 8253-8268; e) S. L. Howell, K. C. Gordon, *J. Phys. Chem. A* **2006**, *110*, 4880-4887; f) C. M. Elliott, E. J. Hershenhart, *J. Am. Chem. Soc.* **1982**, *104*, 7519-7526; g) M. Wachtler, M. Maiuri, D. Brida, J. Popp, S. Rau, G. Cerullo, B. Dietzek, *ChemPhysChem* **2013**, *14*, 2973-2983.

[12] O. Mongin, P. Rocca, L. Thomas-dit-Dumont, F. Trécourt, F. Marsais, A. Godard, G. Quéguiner, *J. Chem. Soc., Perkin Trans. 1* **1995**, 2503-2508.

[13] a) M. J. Fuentes, R. J. Bognanno, W. G. Dougherty, W. J. Boyko, W. S. Kassel, T. J. Dudley, J. J. Paul, *Dalton Trans.* **2012**, *41*, 12514-12523; b) S. Klein, W. G. Dougherty, W. S. Kassel, T. J. Dudley, J. J. Paul, *Inorg. Chem.* **2011**, *50*, 2754-2763.

[14] Y. Takuma, Y. Kasuga in *Production of 2-chloro-5-hydroxypyridine, Mitsubishi Chem. Corp., Patent IPC: C07B61/00 C07D213/65*, *Vol.* Mitsubishi Chem. Corp., **1998**.

[15] M. Ando, N. Sato, T. Nagase, K. Nagai, S. Ishikawa, H. Takahashi, N. Ohtake, J. Ito, M. Hirayama, Y. Mitobe, H. Iwaasa, A. Gomori, H. Matsushita, K. Tadano, N. Fujino, S. Tanaka, T. Ohe, A. Ishihara, A. Kanatani, T. Fukami, *Bioorg. Med. Chem.* **2009**, *17*, 6106-6122.

[16] S. D. Kuduk, R. M. DiPardo, M. G. Bock, *Org. Lett.* **2005**, *7*, 577-579.

[17] a) A. Jutand, A. Mosleh, *J. Org. Chem.* **1997**, *62*, 261-274; b) S. A. McFarland, F. S. Lee, K. Cheng, F. L. Cozens, N. P. Schepp, *J. Am. Chem. Soc.* **2005**, *127*, 7065-7070.

[18] C. M. Elliott, R. A. Freitag, D. D. Blaney, *J. Am. Chem. Soc.* **1985**, *107*, 4647-4655.

[19] A. Juris, V. Balzani, P. Belser, A. Von Zelewsky, *Helv. Chim. Acta* **1981**, *64*, 2175-2182.

[20] S. J. Slattery, N. Gokaldas, T. Mick, K. A. Goldsby, *Inorg. Chem.* **1994**, *33*, 3621-3624.

[21] V. V. Pavlishchuk, A. W. Addison, *Inorg. Chim. Acta* **2000**, *298*, 97-102.

[22] K. Suzuki, A. Kobayashi, S. Kaneko, K. Takehira, T. Yoshihara, H. Ishida, Y. Shiina, S. Oishic, S. Tobita, *Phys. Chem. Chem. Phys.* **2009**, *11*, 9850-9860.

[23] a) A. A. Abdel-Shafi, D. R. Worrall, A. Y. Ershov, *Dalton Trans.* **2004**, 30-36; b) J. Hankache, M. Niemi, H. Lemmetyinen, O. S. Wenger, *Inorg. Chem.* **2012**, *51*, 6333-6344.

[24] a) A. Yoshimura, M. Z. Hoffman, H. Sun, *J. Photochem. Photobiol. A* **1993**, *70*, 29-33; b) P. Müller, K. Brettel, *Photochem. Photobiol. Sci.* **2012**, *11*, 632-636.

[25] D. M. Roundhill, *Photochemistry and Photophysics of Metal Complexes*, Plenum Press, New York, **1994**, p.

[26] C. R. Bock, J. A. Connor, A. R. Gutierrez, T. J. Meyer, D. G. Whitten, B. P. Sullivan, J. K. Nagle, *J. Am. Chem. Soc.* **1979**, *101*, 4815-4824.

[27] A. El-ghayoury, A. Harriman, R. Ziessel, *Chem. Commun.* **1999**, 2027-2028.

[28] W. Sattler, L. M. Henling, J. R. Winkler, H. B. Gray, *J. Am. Chem. Soc.* **2015**, *137*, 1198-1205.

[29] D. C. Smith, H. B. Gray, *Coord. Chem. Rev.* **1990**, *100*, 169-181.

[30] D. Shukla, R. H. Young, S. Farid, *J. Phys. Chem. A* **2004**, *108*, 10386-10394.

[31] a) K. T. Tarantino, P. Liu, R. R. Knowles, *J. Am. Chem. Soc.* **2013**, *135*, 10022-10025; b) H. G. Yayla, R. R. Knowles, *Synlett* **2014**, *25*, 2819-2826.

[32] S. Fukuzumi, K. Ishikawa, K. Hironaka, T. Tanaka, *J. Chem. Soc., Perkin Trans. 2* **1987**, 751-760.

[33] S. K. Ghoshal, S. K. Sarkar, G. S. Kastha, *Bull. Chem. Soc. Jpn.* **1981**, *54*, 3556-3561.

[34] H. Lutz, E. Breheret, L. Lindqvist, *J. Phys. Chem.* **1973**, *77*, 1758-1762.

[35] a) L. Biczok, N. Gupta, H. Linschitz, *J. Am. Chem. Soc.* **1997**, *119*, 12601-12609; b) L. Biczók, H. Linschitz, *J. Phys. Chem.* **1995**, *99*, 1843-1845; c) J. Nomrowski, O. S. Wenger, *Inorg. Chem.* **2015**, *54*, 3680-3687.

[36] J. T. Muckerman, J. H. Skone, M. Ning, Y. Wasada-Tsutsui, *Biochim. Biophys. Acta* **2013**, *1827*, 882-891.

[37] a) J. J. Warren, T. A. Tronic, J. M. Mayer, *Chem. Rev.* **2010**, *110*, 6961-7001; b) D. R. Weinberg, C. J. Gagliardi, J. F. Hull, C. F. Murphy, C. A. Kent, B. C. Westlake, A. Paul, D. H. Ess, D. G. McCafferty, T. J. Meyer, *Chem. Rev.* **2012**, *112*, 4016-4093; c) S. Y. Reece, D. G. Nocera, *Annu. Rev. Biochem.* **2009**, *78*, 673-699; d) C. Costentin, M. Robert, J.-M. Savéant, *Acc. Chem. Res.* **2010**, *43*, 1019-1029; e) L. Hammarström, S. Styring, *Energy Environ. Sci.* **2011**, *4*, 2379-2388; f) T. T. Eisenhart, J. L. Dempsey, *J. Am. Chem. Soc.* **2014**, *136*, 12221-12224; g) T. Irebo, M.-T. Zhang, T. F. Markle, A. M. Scott, L. Hammarström, *J. Am. Chem. Soc.* **2012**, *134*, 16247–16254.

[38] C. R. Waidmann, A. J. M. Miller, C. W. A. Ng, M. L. Scheuermann, T. R. Porter, T. A. Tronic, J. M. Mayer, *Energy Environ. Sci.* **2012**, *5*, 7771-7780.

[39] Bruker Analytical X-ray Systems Inc., *Apex2* **2006**, *Version 2 User Manual*, M86-E01078, Madison, WI.

[40] L. Palatinus, G. Chapuis, *J. Appl. Crystallogr.* **2007**, *40*, 786-790.

[41] P. W. Betteridge, J. R. Carruthers, R. I. Cooper, K. Prout, D. J. Watkin, *J. Appl. Crystallogr.* **2003**, *36*, 1487-1487.

[42] C. F. Macrae, I. J. Bruno, J. A. Chisholm, P. R. Edgington, P. McCabe, E. Pidcock, L. Rodriguez-Monge, R. Taylor, J. van de Streek, P. A. Wood, *J. Appl. Crystallogr.* **2008**, *41*, 466-470.

FULL PAPER

A fourfold methoxy-substituted 2,2'-bipyridine was used a ligand for homoleptic complexes with Fe(II), Ru(II), and Os(II). The latter two are strong electron donors in their long-lived ^{3}MLCT excited states. Their ability to act as photoredox reagents in acidic media has been demonstrated on the example of acetophenone reduction via proton-could electron transfer (PCET).

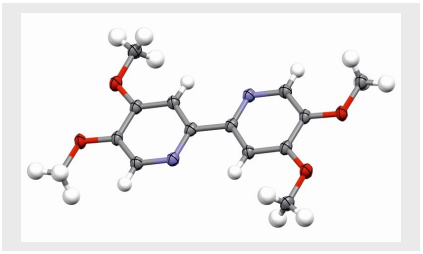

Photoredox Catalysts

*Laura A. Büldt, Alessandro Prescimone, Markus Neuburger, Oliver S. Wenger**

Page No. – Page No.

Photoredox Properties of Homoleptic d^6 Metal Complexes with the Electron-Rich 4,4',5,5'-Tetramethoxy-2,2'-Bipyridine Ligand